JCI The Journal of Clinical Investigation

HTLV-1 propels untransformed CD4$^+$ lymphocytes into the cell cycle while protecting CD8$^+$ cells from death

David Sibon, … , Franck Mortreux, Eric Wattel

J Clin Invest. 2006;116(4):974-983. https://doi.org/10.1172/JCI27198.

Research Article Immunology

Human T cell leukemia virus type 1 (HTLV-1) infects both CD4$^+$ and CD8$^+$ lymphocytes, yet it induces adult T cell leukemia/lymphoma (ATLL) that is regularly of the CD4$^+$ phenotype. Here we show that in vivo infected CD4$^+$ and CD8$^+$ T cells displayed similar patterns of clonal expansion in carriers without malignancy. Cloned infected cells from individuals without malignancy had a dramatic increase in spontaneous proliferation, which predominated in CD8$^+$ lymphocytes and depended on the amount of tax mRNA. In fact, the clonal expansion of HTLV-1–positive CD8$^+$ and CD4$^+$ lymphocytes relied on 2 distinct mechanisms — infection prevented cell death in the former while recruiting the latter into the cell cycle. Cell cycling, but not apoptosis, depended on the level of viral-encoded tax expression. Infected *tax*-expressing CD4$^+$ lymphocytes accumulated cellular defects characteristic of genetic instability. Therefore, HTLV-1 infection establishes a preleukemic phenotype that is restricted to CD4$^+$ infected clones.

 Related Commentary, page 858

HTLV-1 propels untransformed CD4+ lymphocytes into the cell cycle while protecting CD8+ cells from death

David Sibon,[1,2] Anne-Sophie Gabet,[1] Marc Zandecki,[3] Christiane Pinatel,[1] Julien Thête,[1] Marie-Hélène Delfau-Larue,[4] Samira Rabaaoui,[1] Antoine Gessain,[5] Olivier Gout,[6] Steven Jacobson,[7] Franck Mortreux,[1] and Eric Wattel[1,2]

[1]Oncovirologie et Biothérapies, CNRS UMR5537 — Université Claude Bernard, Centre Léon Bérard, Lyon, France. [2]Service d'Hématologie, Hôpital Edouard Herriot, Lyon, France. [3]Laboratoire d'Hématologie, Centre Hospitalier Universitaire (CHU) d'Angers, Angers, France. [4]Laboratoire d'Immunologie, CHU Henri Mondor, Créteil, France. [5]Unité d'Epidémiologie et Physiopathologie des Virus Oncogènes, Institut Pasteur, Paris, France. [6]Service de Neurologie, Fondation Rothschild, Paris, France. [7]Viral Immunology Section, Neuroimmunology Branch, National Institute of Neurological Disorders and Stroke, National Institutes of Health, Bethesda, Maryland, USA.

Human T cell leukemia virus type 1 (HTLV-1) infects both CD4+ and CD8+ lymphocytes, yet it induces adult T cell leukemia/lymphoma (ATLL) that is regularly of the CD4+ phenotype. Here we show that in vivo infected CD4+ and CD8+ T cells displayed similar patterns of clonal expansion in carriers without malignancy. Cloned infected cells from individuals without malignancy had a dramatic increase in spontaneous proliferation, which predominated in CD8+ lymphocytes and depended on the amount of *tax* mRNA. In fact, the clonal expansion of HTLV-1–positive CD8+ and CD4+ lymphocytes relied on 2 distinct mechanisms — infection prevented cell death in the former while recruiting the latter into the cell cycle. Cell cycling, but not apoptosis, depended on the level of viral-encoded *tax* expression. Infected *tax*-expressing CD4+ lymphocytes accumulated cellular defects characteristic of genetic instability. Therefore, HTLV-1 infection establishes a preleukemic phenotype that is restricted to CD4+ infected clones.

Introduction

Gaining access to the early molecular and cellular events governing malignant transformation in vivo is of considerable interest for understanding and targeting tumor development. Deltaretrovirus infection constitutes an exceptional system for exploring early oncogenesis in vivo (1) and in vitro (2). Deltaretroviruses include human T cell leukemia virus (HTLV) types 1 (3) and 2 (HTLV-1 and -2; ref. 4), the recently discovered HTLV-3 (5) and -4 (6), simian T cell leukemia viruses (7), and the bovine leukemia virus (8). These lymphotropic retroviruses infect vertebrates in whom they cause leukemia and lymphomas; HTLV-1, for instance, is associated with adult T cell leukemia/lymphoma (ATLL) (9). Deltaretrovirus-associated lymphoid malignancies regularly occur after a prolonged period of latency. Some of these viruses may also cause inflammatory diseases such as HTLV-1–associated myelopathy/tropical spastic paraparesis (HAM/TSP) (10), uveitis (11), and infective dermatitis in the case of HTLV-1 (12).

At the molecular level, the oncogenicity of deltaretroviruses mainly depends on the expression of viral oncoproteins possessing a pleiotropic effect on the cellular metabolism. By interfering with genome repair, cell cycle, and apoptosis, the HTLV-1–encoded Tax oncoprotein plays a central role in the clonal expansion and genetic instability of infected cells and thereby in HTLV-1–associated leukemogenesis (2, 13). Importantly, as ATLL cells do not express Tax (14–16), the oncogenic effect of Tax expression is necessarily restricted to the premalignant phase of the infection. For all deltaretroviruses, this preleukemic phase includes the persistent clonal expansion of infected cells that frequently express viral oncoproteins (16). In vivo it is possible to identify the premalignant clone (i.e., the infected clone that will ultimately become transformed at the tumor stage) on the basis of its early detection and its high level of clonal expansion and genetic instability (1). It is also possible ex vivo, by limiting dilution cloning of PBMCs, to access premalignant cells and to compare their properties with those of uninfected cells deriving from the same infected organism (17–19).

Although HTLV-1 infects both CD4+ and CD8+ T cells (20–22), ATLL is regularly of the CD4+ phenotype (23), meaning that the leukemogenic potential of the virus is restricted to the CD4+ subset. On the contrary, both CD4+ and CD8+ lymphocytes are involved in the immunological control of the infection and in the inflammatory processes that govern the pathogeny of HAM/TSP, uveitis and infectious dermatitis (24–26). CD4+ lymphocytes infected by coculture with an HTLV-1 cell line display a significantly higher viral transcription rate than CD8+ cells infected with the same procedure (27), suggesting that the T cell phenotype itself, probably via transcription factor availability, influences viral transcription and replication. In vitro, a high level of spontaneous proliferation characterizes PBMCs from HTLV-1–infected individuals (28). Whether this correlates with the clonal expansion of both infected subsets in vivo has not been investigated to date. Altered growth kinetics is characteristic of cloned cells naturally infected by HTLV-1 (17) and might result from cell cycle and/or apoptosis dysfunctions.

Nonstandard abbreviations used: ATLL, adult T cell leukemia/lymphoma; HAM/TSP, HTLV-1–associated myelopathy/tropical spastic paraparesis; HTLV, human T cell leukemia virus; IPCR, inverse PCR; PHA, phytohemagglutinin; PI, propidium iodide.

Conflict of interest: The authors have declared that no conflict of interest exists.

Citation for this article: *J. Clin. Invest.* **116**:974–983 (2006). doi:10.1172/JCI27198.

Table 1
Patient characteristics

Patient	Sex	Age (yr)	Native country	EDSS	Duration of illness (yr)
Patient 1	F	38	Chad	6.5	3
Patient 2	M	61	France	6	5
Patient 3 (DO45)	F	44	Martinique	4.5	4
Patient 4 (SI88)	F	50	Martinique	4.5	3
Patient 5	F	45	Martinique	1	1
Patient 6	M	49	United States	8	6
Patient 7	M	59	Jamaica	7	10
Patient 8	M	59	United States	7	14
Patient 9	F	55	Jamaica	7.5	26

Neurologic impairment was evaluated using the expanded disability status scale (EDSS). F, female; M, male.

Here we have investigated the pattern of HTLV-1 replication in $CD4^+$ versus $CD8^+$ infected lymphocytes in vivo. We have shown that in the absence of malignancy, both infected $CD4^+$ and $CD8^+$ T cells displayed a pattern of clonal expansion in vivo. We next designed a cellular model of HTLV-1 replication through clonal expansion in order to investigate the mechanisms underlying clonal proliferation in the 2 lymphocyte subsets. We analyzed the effect of the infection on cell cycle and apoptosis in cloned $CD4^+$ and $CD8^+$ cells from infected individuals. In the absence of malignancy, the increased degree of infected T cell proliferation was shown to result from 2 clearly distinct mechanisms with respect to the T cell phenotype. Together with the presence of multiple $CD4^+$-restricted cellular defects characteristic of genetic instability, these findings contribute to establishing the existence of a $CD4^+$-restricted preleukemic phenotype.

Results

Cellular phenotype and HTLV-1 proviral loads in vivo. $CD4^+$ and $CD8^+$ T lymphocytes express GLUT-1 (29), a receptor for HTLV-1, and represent the reservoir for HTLV-1 in vivo (19–21, 28). To better assess HTLV-1 replication in the 2 lymphocyte subsets, we first compared HTLV-1 proviral loads between $CD4^+$ and $CD8^+$ T cells. To this end, we enriched the cellular fraction in $CD4^+CD8^-$ and $CD4^-CD8^+$ T cells by negative selection as described in Methods. For this experiment we used 9 samples derived from 9 patients with HAM/TSP. Pertinent clinical data accompanying the DNA samples are shown in Table 1. After negative selection with the human $CD4^+$ enrichment cocktail, the mean purity of $CD4^+$ T cells and the mean $CD8^+$ T cell contamination were 94% and 0.02%, respectively. After negative selection with the human $CD8^+$ enrichment cocktail, the mean purity of $CD8^+$ T cells and the mean $CD4^+$ T cell contamination were 85% and 0%, respectively. Quantitative PCR was carried out as described in Methods. As shown in Figure 1A, proviral loads of $CD4^+$ lymphocytes ranged from 13 to 140 copies per 100 cells (mean, 61.8; median, 54.5) while those of the $CD8^+$ subset were significantly lower, ranging from 4.7 to 32.3 per 100 cells (mean, 24.7; median, 26.6; $P = 0.016$; Student's t test for independent samples). These results indicate that in HAM/TSP the proviral loads of $CD4^+$ cells are significantly higher than those of $CD8^+$ lymphocytes.

Clonal expansion of $CD4^+$ and $CD8^+$ HTLV-1–positive cells in vivo. $CD4^+$ and $CD8^+$ T cells from patients with HAM/TSP are characterized by high spontaneous proliferation ex vivo, which is particularly important in $CD8^+$ cells (28). In vivo, TCR analyses have

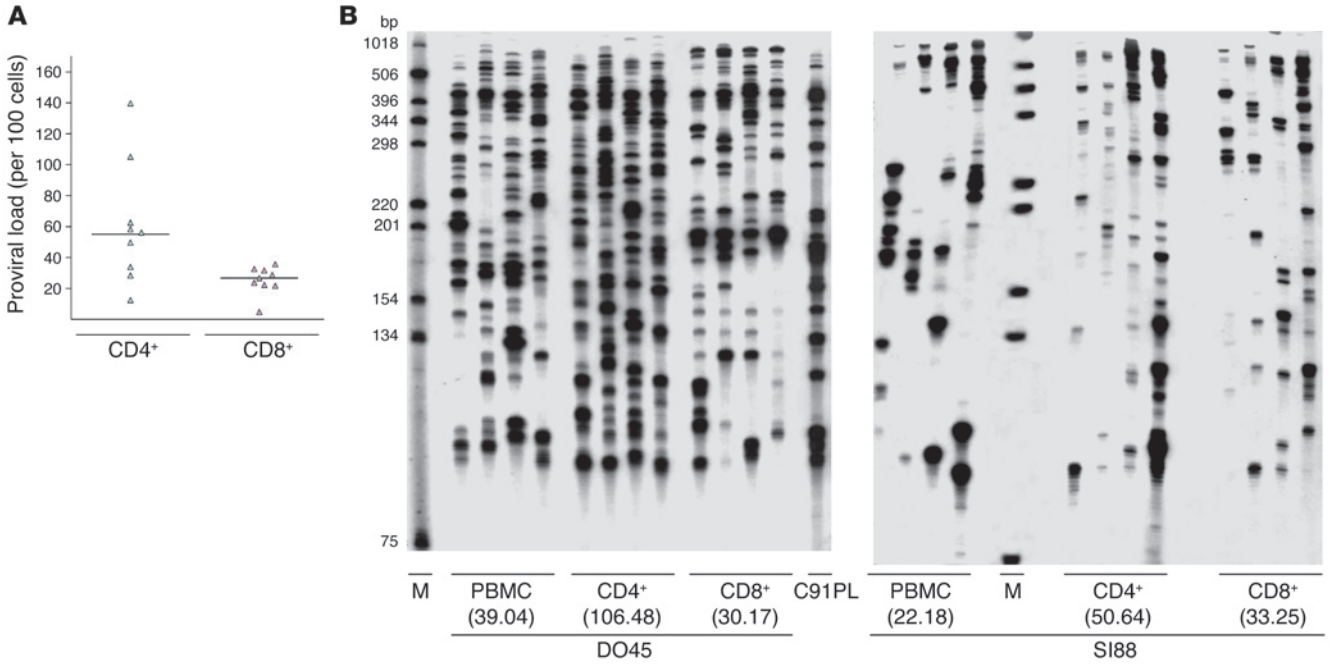

Figure 1
Proviral loads (**A**) and clonality (**B**) of HTLV-1–positive cells in highly purified $CD4^+CD8^-$ and $CD4^-CD8^+$ lymphocytes from HAM/TSP patients DO45 and SI88 (see Table 1). The clonal distribution of integrated HTLV-1 sequences within the DNA of $CD4^+$ and $CD8^+$ cells was assessed by quadruplicate IPCR experiments as described in Methods. Numbers in parentheses represent the proportion of infected cells as evidenced by real-time quantitative PCR. M, molecular weight marker. C91PL is an HTLV-1 cell line used as positive control.

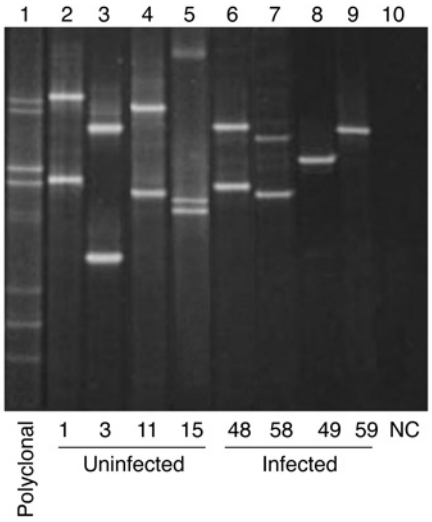

Figure 2
Multiplex PCR-γ denaturing gradient gel electrophoresis analysis of TCR rearrangement in human T cell clones. Each lane represents the migration of the PCR product of 1 clone. Clones are identified by their unique clone number (bottom). Samples with 1 (lanes 8 and 9) or 2 (lanes 2–4, 6, and 7) signals correspond with mono- or biallelic rearrangements, respectively. Sample with 3 bands (lane 5) corresponds to a biallelic rearrangement with a heteroduplex. A polyclonal sample is shown on lane 1; lane 10 correspond to a negative control (NC).

demonstrated that both $CD4^+$ and $CD8^+$ cells undergo a pattern of clonal expansion (30–34). However, these experiments did not take into account the infected versus uninfected nature of ex vivo and in vivo expanded $CD4^+$ and $CD8^+$ cells. Knowing that clonal expansion is the rule for HTLV-1–infected cells in vivo (16, 30, 35–44), we investigated the distribution of HTLV-1–integrated sequences within the DNA of the 2 lymphocyte subsets by amplifying HTLV-1 3′ extremities together with their cellular flanking sequences. The same samples from 9 HAM/TSP patients used for quantitative PCR were assayed for inverse PCR (IPCR). Typical IPCR results are shown in Figure 1B. As previously described, a pattern of clonal expansion of HTLV-1–positive cells was apparent in all PBMC samples. Furthermore, clones of HTLV-1–positive cells were found in both $CD4^+$ and $CD8^+$ T cells (Figure 1B), demonstrating for the first time to our knowledge that both subsets of infected lymphocytes undergo clonal expansion. This was true for all patients studied. As there is a stochastic element to IPCR amplification of low-frequency HTLV-1 integration sites, quadruplicate IPCR analysis was performed (4×0.5 μg, ~$4 \times 75 \times 10^3$ cell equivalents) on the 27 samples derived from the 9 patients. A signal present in all 4 samples corresponded to a clonal frequency of ≥1 in 150 cells, while a single positive amplification corresponded to a frequency of ≤1 in 1,500. After quadruplicate experiments, the mean number of infected clones was significantly higher in $CD4^+$ than in $CD8^+$ cells: 73.5 versus 57 per 2 μg DNA ($P = 0.008$; *t* test for independent samples). The proportion of clones with a clonal frequency between 1 in 1,500 and 1 in 300 (i.e., detected 1 and 2 times after quadruplicate IPCR experiments) was not significantly different between the 2 subsets of T cells. In contrast, the clonal proportion of more than 1 in 300 infected cells (i.e., detected 3 and 4 times after quadruplicate IPCR experiments) was significantly higher in $CD4^+$ cells: 16 versus 8.5 ($P = 0.032$; *t* test for independent samples). For both T cell subsets, proviral loads positively correlated with the number of abundant clones, i.e., those detected 3 times or more after quadruplicate IPCR and having a clonal frequency of more than 1 in 300 infected cells. In contrast, proviral loads negatively correlated with the number of low abundant clones, i.e., those detected less than 3 times after quadruplicate IPCR and having a clonal frequency of less than 1 in 300 infected cells. Thus for both subsets of infected lymphocytes, proviral loads depended more on the degree of clonal expansion than on the number of infected clones. Therefore the previously described pattern of HTLV-1 clonal expansion pertains to both $CD4^+$ and $CD8^+$ infected lymphocytes in vivo, the $CD4^+$ subset having a significantly higher degree of cellular expansion than the $CD8^+$ subset, allowing for higher proviral loads in $CD4^+$ cells.

A cellular model of HTLV-1 replication via clonal expansion ex vivo. Although both T cell subsets undergo clonal expansion, ATLL is predominantly of the $CD4^+$ phenotype. As ATLL onset is the consequence of prolonged T cell infection (16, 45), we hypothesized that distinct mechanisms might underlie infected T cell expansion in the 2 lymphocyte subsets. Schematically, cell accumulation and cell proliferation represent the 2 main mechanisms contributing to clonal expansion; the former relies on the regulation of apoptosis, while the latter relies on the regulation of the cell cycle. We therefore designed a cellular model of HTLV-1 replication via clonal expansion in order to compare the effect of HTLV-1 infection on apoptosis and cell cycle in $CD4^+$ versus $CD8^+$ cells. To this end, T cell–limiting dilution cloning of PBMCs from 4 HAM/TSP patients allowed us to clone uninfected and naturally infected $CD4^+$ and $CD8^+$ cells from the same infected individuals. A total of 22 uninfected clones (12 $CD4^+$) and 44 infected clones (29 $CD4^+$) deriving from the 4 patients with HAM/TSP were studied in detail. Infected and uninfected clones were not immortalized and required IL-2 and stimulation with phytohemagglutinin (PHA) and feeder cells at 14-day intervals for continued growth. All 66 clones harbored distinct and unique TCRs, as evidenced by multiplex PCR-γ denaturing gradient gel electrophoresis (Figure 2). Among the 44 infected clones tested, 31 expressed p19, including 21 $CD4^+$ (~72%) and 10 $CD8^+$ (~67%) clones. The HTLV-1 *tax* mRNA load was determined by diluting the cDNA extracted from cells of the HTLV-1–infected MT-4 cell line. This allowed for determination of the sensitivity of the real-time RT-PCR assay. The detection threshold was 250×10^{-5} ng diluted in 25 μl water. In 34 of the 37 HTLV-1–infected clones screened (~92%) the amount of *tax* mRNA was above this threshold, including 22 of 24 $CD4^+$ (~92%) and 12 of 13 $CD8^+$ clones (~92%), as evidenced by quantitative real-time RT-PCR. The HTLV-1 *tax* mRNA load ranged from less than 250×10^{-5} to 603,475 AU (median, 35,208; mean ± SEM, 128,480 ± 29,123) without significant difference between $CD4^+$ (median, 64,175; mean ± SEM, 137,520 ± 35,994) and $CD8^+$ clones (median, 23,821; mean ± SEM, 111,790 ± 51,202). There was a significant correlation between *tax* mRNA loads and the level of p19 expression as measured by ELISA ($P < 10^{-4}$; r, ~0.6246, Spearman rank correlation).

Infected $CD4^+$ clones frequently display multinucleated cells with nuclear abnormalities. Cell morphology was analyzed on all infected and uninfected clones, and some differences clearly distinguished the former from the latter (Figure 3). In infected clones, 38% had dedifferentiated lymphocytes, whereas uninfected clones had none

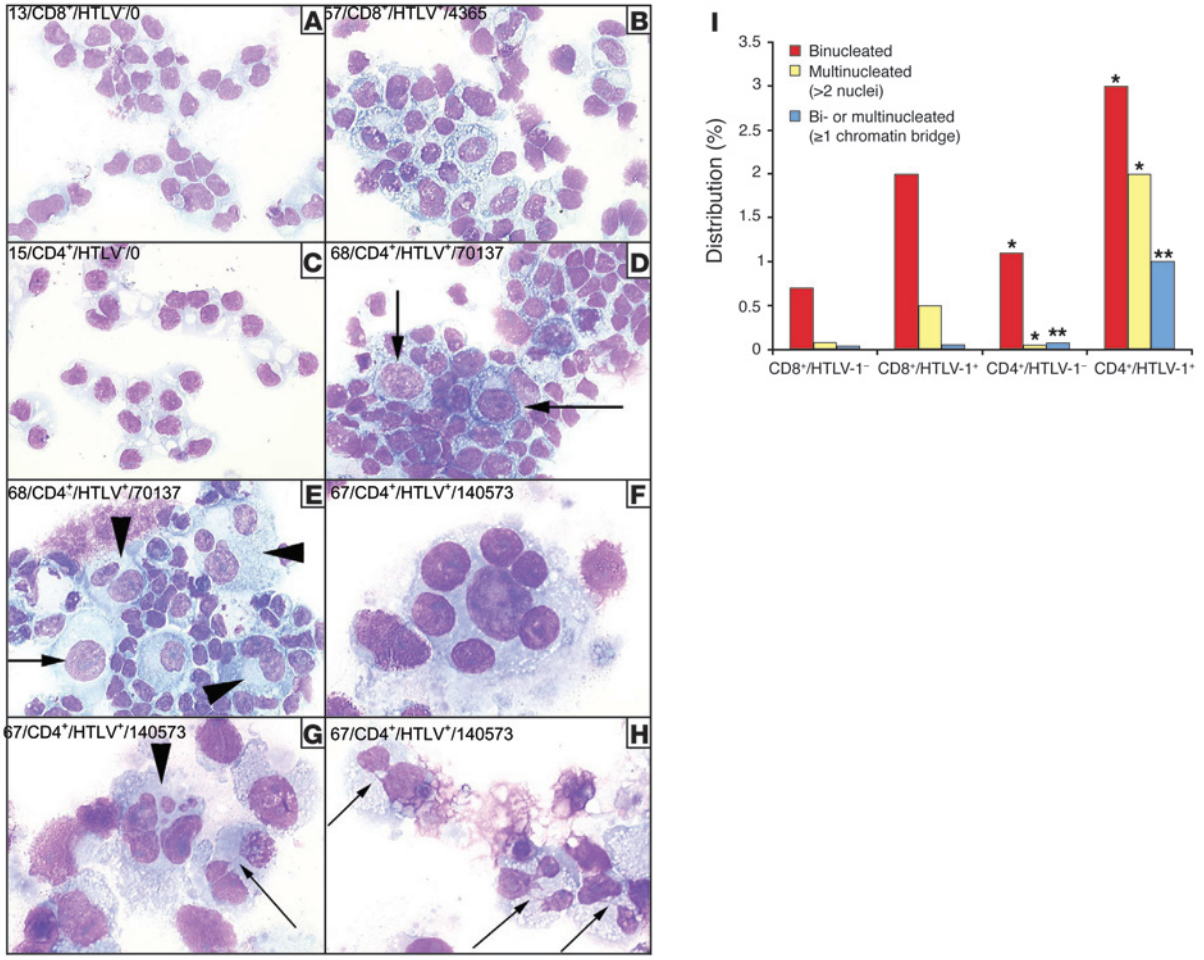

Figure 3
Infected CD4+ lymphocytes that express *tax* display both nuclear abnormalities and cytokinesis defects. Clones 13 (**A**), 15 (**C**), 57 (**B**), 67 (**F**–**H**), and 68 (**D** and **E**) were cytospun, fixed, and stained with May-Grünwald and Giemsa. Label notation indicates the unique clone number, the phenotype, the infected or uninfected nature of the cells, and the corresponding amount of *tax* mRNA, measured in arbitrary units. Compared with uninfected CD8+ clones (**A**), HTLV-1–positive CD8+ clones (**B**) displayed enlarged cells with enlarged cytoplasm. Compared with uninfected CD4+ clones (**C**), HTLV-1–positive CD4+ clones (**D** and **E**) frequently display giant cells, some harboring enlarged nucleus (arrows). Multinucleated cells frequently displayed nuclei of heterogeneous sizes, as identified by arrowheads in **E** and **G** and shown at higher magnification in **F**. Chromatin bridges connecting nuclei in multinucleated cells are identified by smaller arrows in **G** and **H**. The distribution of cellular nuclearity according to phenotype and infectious status is shown in **I**. *$P < 0.001$; **$P < 0.0001$, infected vs. uninfected cells. Magnification, ×40 (**A**–**E**), ×100 (**F**–**H**).

($P = 0.03$). Binucleated and multinucleated cells with enlarged cytoplasm were significantly more frequent in infected clones than in uninfected clones (3.9% versus 0.9%; $P < 10^{-4}$). The majority of multinucleated cells displayed well-separated nuclei (Figure 3F), whereas chromatin bridges connected nuclei in some clones (Figure 3, G and H). Cells with enlarged nuclei were also more frequent among infected clones (1.1% versus 0.3%; $P = 0.005$). Interestingly, multinuclearity and impaired cytokinesis significantly predominated in CD4+ infected clones, whereas the presence of chromatin bridges was almost exclusively restricted to CD4+ clones (Figure 3I). The degree of *tax* expression significantly correlated to the proportion of binucleated ($P = 0.041$; r, ~0.4246, Spearman rank correlation) and multinucleated cells ($P = 0.007$; r, ~0.5350, Spearman rank correlation). Together these results indicate that a significant proportion of *tax*-expressing CD4+ lymphocytes naturally infected by full-length viruses fail to undergo proper cytokinesis and cell division, resulting in the formation of multinucleated giant cells.

Altered growth kinetics of HTLV-1–infected CD4+ and CD8+ cell clones. Ex vivo, we first investigated the kinetics of IL-2–dependent and spontaneous clonal proliferation of CD4+ and CD8+ infected clones. For each clone, IL-2–dependent proliferation was assessed by measuring cell count (Figure 4, A and B) and ^{3}H-thymidine incorporation (Figure 4, C and D) in the presence of IL-2. The growth kinetics of the entire collection of 66 clones are represented in Figure 4. As shown in Figure 4A, the degree of cell proliferation was significantly higher in infected than in uninfected T cell clones. The difference was statistically significant at day 13 after PHA stimulation. Over the course of the experiment, the positive effect of the infection on cell count was significantly higher in CD8+ than in CD4+ lymphocytes (Figure 4B). The difference between infected and uninfected clones was statistically significant for CD8+ cells at days 7 ($P = 0.04$), 10 ($P = 0.04$), and 13 ($P = 0.002$), whereas CD4+ cells significantly outgrew their uninfected counterparts only at day 13 ($P = 0.04$). No significant correlation was

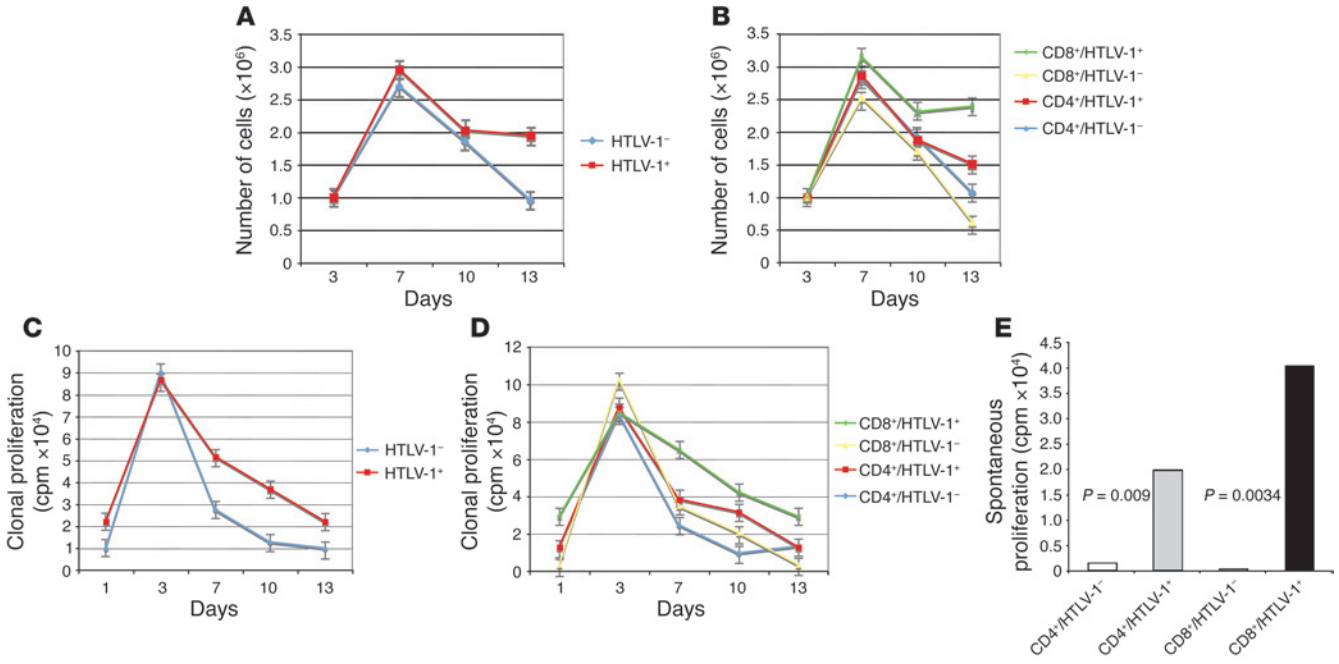

Figure 4
Altered growth kinetics of CD4⁺ and CD8⁺ HTLV-1–infected clones. Sixty-six clones were analyzed. (**A**) Increased growth of HTLV-1–infected clones. (**B**) Increased growth of CD4⁺ and CD8⁺ HTLV-1–infected clones. (**C**) Kinetics of IL-2–dependent clonal proliferation of infected and uninfected clones. (**D**) Kinetics of IL-2–dependent clonal proliferation of infected and uninfected CD4⁺ and CD8⁺ clones. (**E**) Spontaneous clonal proliferation of infected and uninfected CD4⁺ and CD8⁺ clones.

noted between *tax* mRNA load and cell count. Even so, there was a trend for a negative correlation between the 2 values at day 10 ($P = 0.059$; r, ~–0.3829, Spearman rank correlation). For CD4⁺ cells, the mean ^{3}H-thymidine incorporation of infected clones was 1-, 2-, 3-, and 1-fold higher (mean, 1.6-fold) than that of uninfected clones at days 3, 7, 10, and 13, respectively. The difference between infected and uninfected CD4⁺ cells was statistically significant at day 10 ($P = 0.05$). It is notable that at the same time the degree of cell proliferation was identical between infected and uninfected CD4⁺ clones (Figure 4B), suggesting that infected CD4⁺ cells display an increase of DNA synthesis in the absence of cell division, a result consistent with the high frequency of multinucleated cells in infected CD4⁺ clones. For CD8⁺ cells, the mean ^{3}H-thymidine incorporation of infected clones was 1-, 2-, 2-, and 9-fold higher than that of uninfected clones at days 3, 7, 10, and 13, respectively (mean, 4-fold). The difference between infected and uninfected CD8⁺ cells was statistically significant at days 7 ($P = 0.03$), 10 ($P = 0.03$), and 13 ($P = 0.05$). At day 13, ^{3}H-thymidine incorporation positively correlated with *tax* expression ($P = 0.017$; r, ~0.6264, Spearman rank correlation), whereas no statistically significant correlation was observed at days 3, 7, and 10.

We next compared the effect of HTLV-1 on spontaneous proliferation between CD4⁺ and CD8⁺ lymphocytes. In the absence of IL-2, the mean ^{3}H-thymidine incorporation of the 44 infected clones was approximately 20-fold higher than that of the 22 uninfected clones ($P = 0.002$, Mann-Whitney test). Figure 4E shows that both CD4⁺ and CD8⁺ infected clones displayed a significantly higher degree of spontaneous proliferation than their uninfected counterparts, the ^{3}H-thymidine incorporation increase being significantly higher for CD8⁺ (56-fold) than for CD4⁺ infected cells (11-fold; Figure 4E). For the 44 HTLV-1–infected clones, the degree of spontaneous proliferation correlated with the *tax* mRNA load ($P = 0.001$; r, ~0.6842, Spearman rank correlation). Twenty-one additional clones were generated by limiting dilution cloning of PBMCs deriving from 2 uninfected blood donors and assayed for spontaneous proliferation. Their mean ^{3}H-thymidine incorporation was of the same order as that of uninfected clones deriving from HTLV-1–infected individuals (3,399 versus 1,519 cpm; P = NS). Together, these results indicate that HTLV-1 infection has a modest positive effect on IL-2–dependent CD4⁺ or CD8⁺ proliferation, which does not depend on *tax* expression. In contrast, the infection appears to strongly affect the spontaneous proliferation of both lymphocyte subsets in a Tax-dependent manner, with a predominant positive effect on the spontaneous proliferation of CD8⁺ cells, which is restricted to infected cells.

Ex vivo, HTLV-1 infection prevents cell death in CD8⁺ lymphocytes while recruiting CD4⁺ lymphocytes into the cell cycle. We next investigated whether the altered growth kinetics of HTLV-1–positive clones relied on distinct effects of the infection on cell death and cell cycle between CD4⁺ and CD8⁺ cells. For all 66 clones, cell death and cell cycle were assessed by flow cytometry at day 6 following PHA stimulation. Representative flow cytometry analyses are shown in Figure 5A, while Figure 5, B and C, represents fluctuations of cell cycle distribution and apoptosis for all 66 infected or uninfected CD4⁺ and CD8⁺ clones. There was no significant difference in cell viability, apoptosis, and necrosis (necrosis and late apoptosis) between HTLV-1–positive and –negative CD4⁺ lymphocytes (Figure 5, A and B). Conversely, cell distribution across the phases of the cell cycle was strongly different between infected and uninfected CD4⁺ lymphocytes (Figure 5B). Overall, the per-

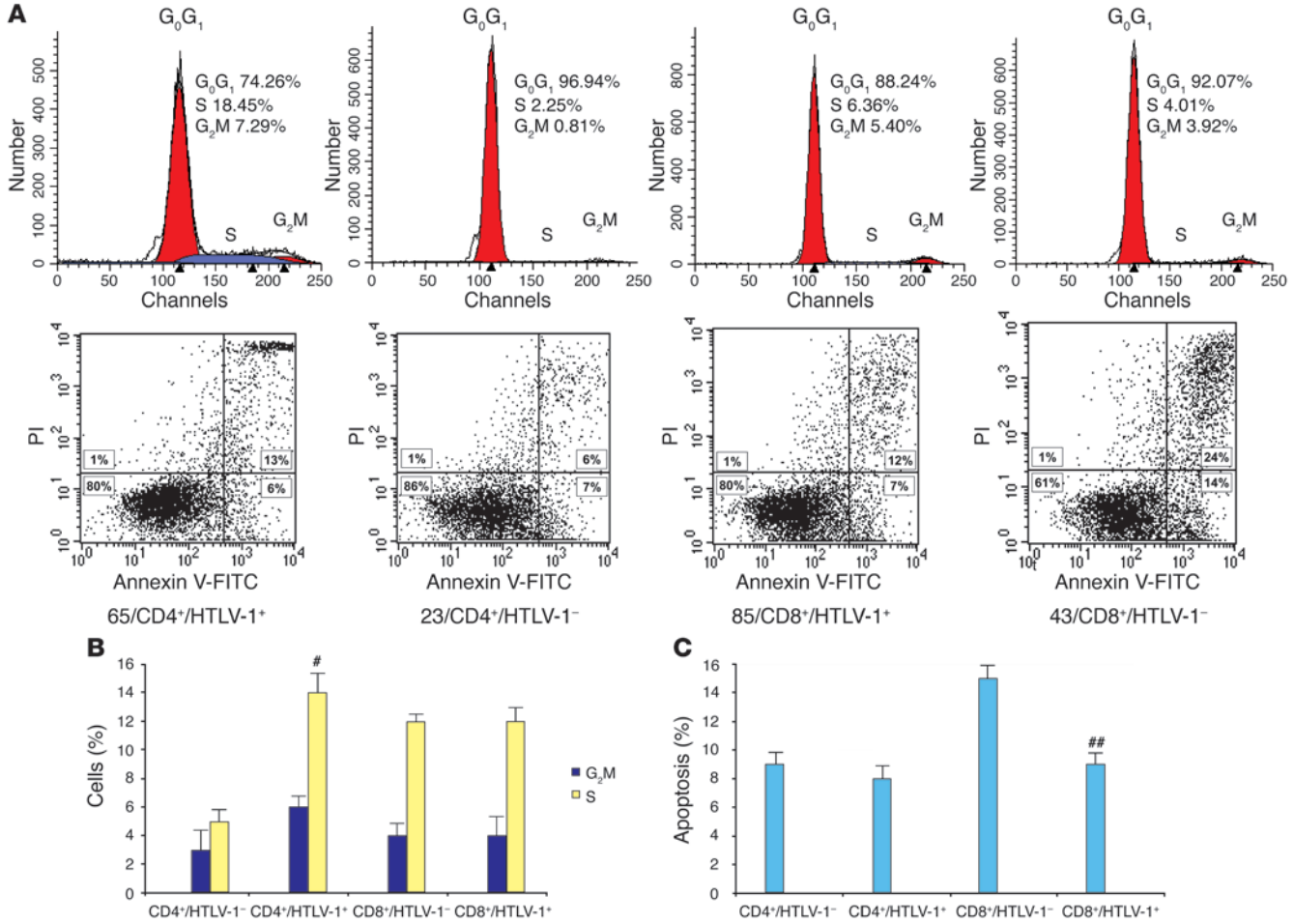

Figure 5
HTLV-1 recruits untransformed CD4+ lymphocytes into the cell cycle while preventing CD8+ cells from cell death. CD4+ and CD8+ clones (66 clones) were analyzed at day 6 from PHA stimulation for cell cycle (**A** and **B**) and apoptosis (**A** and **C**). $^{\#}P = 0.001$, $^{\#\#}P = 0.04$ versus uninfected cells of the same phenotype.

centages of uninfected CD4+ lymphocytes in the G_0G_1, G_2M, and S phases of the cycle were respectively 92%, 3%, and 5%, versus 80%, 6%, and 14% for infected CD4+ lymphocytes ($P = 0.001$, Mann-Whitney test). This result suggests that upon infection, there is a significant redistribution of CD4+ lymphocytes from the G_0G_1 phase toward S and G_2M phases of the cell cycle. In contrast to CD4+ lymphocytes, the percentage of apoptotic cells in infected CD8+ cells was significantly decreased compared with uninfected CD8+ lymphocytes (9% versus 15%; $P = 0.04$, Mann-Whitney test), whereas no significant difference in the distribution across the phases of the cell cycle was noted (Figure 5B). Therefore the clonal expansion of HTLV-1–positive cells relies on 2 distinct mechanisms for CD4+ and CD8+ lymphocytes: infection propels CD4+ lymphocytes through the cell cycle while preventing cell death in CD8+ cells. As Tax is known to interfere with both cell cycle and apoptosis in vitro, we next investigated whether the level of *tax* expression influences these parameters ex vivo in the present model of clonal expansion of cells bearing full-length HTLV-1 proviruses. Overall the *tax* mRNA loads correlated negatively with the percentage of cells in the G_0G_1 phase of the cycle ($P = 0.001$; r, ~–0.5993, Spearman rank correlation) and positively with the percentage of cells in the G_2M and S phases ($P = 0.001$; r, ~0.6021, Spearman rank correlation). These statistically significant correlations were found in both CD4+ and CD8+ clones. In contrast, the level of *tax* expression did not influence apoptosis, necrosis, and cell viability in CD4+ or CD8+ clones.

Discussion

The data presented here show that infected CD4+ and CD8+ cells displayed the same pattern of clonal expansion in vivo. Therefore, both subsets of T cells disseminated the virus at a proviral state, although the degree of clonal expansion was higher in CD4+ than in CD8+ lymphocytes, which accounted for the significantly higher proviral loads harbored by the CD4+ subset of T cells. A cellular model was subsequently designed in order to investigate the mechanisms underlying HTLV-1–dependent cellular expansion in the 2 lymphocyte subsets. Furthermore, as HTLV-1 promotes tumor development rather than maintaining the malignant phenotype (14–16), this cellular model provided an adequate system to study the mechanisms underlying early leukemogenesis. The majority of infected clones was found to express p19 protein and *tax* mRNA without a difference in the frequency and intensity of

expression between CD4+ and CD8+ clones. Thus in the present model the T cell phenotype of naturally infected cells did not influence the level of viral transcription ex vivo.

Multinucleated giant cells, including cells with chromatin bridges, were significantly more frequent in *tax*-expressing cells and culminated in infected CD4+ clones. This suggests that a significant proportion of *tax*-expressing lymphocytes naturally infected by full-length viruses fail to undergo proper cytokinesis and cell division, which results in the formation of multinucleated giant cells. This had been previously described with lymphoid or nonlymphoid cells stably expressing Tax (46, 47). Chromatin bridges, restricted here to CD4+ infected cells, are related to abnormal chromosomal segregation and contribute to genetic instability (48–51). As with anaphase bridges histologically observed in solid tumors (48–53), these abnormalities are thought to rely on telomere dysfunction and thereby constitute a harbinger of subsequent malignant transformation, since they reflect oncogenic chromosome rearrangements (48). We previously demonstrated that transient Tax overexpression downregulates telomerase activity (54), which is consistent with our present findings and suggests that chromatin bridges, which are restricted to multinucleated infected CD4+ lymphocytes expressing *tax*, are the consequence of Tax-related telomere attrition. Alternatively, stable expression of Tax stably activates *human telomerase reverse transcriptase* (*hTERT*) gene expression (55). However, it was recently shown that stable *hTERT* expression possesses a specific effect in CD4+ cells, namely the promotion of telomere dysfunction leading to chromatin bridges (56).

IL-2–dependent cell proliferation and ^{3}H-thymidine incorporation were found to be higher in infected than in uninfected clones. The positive effect of the infection on cell proliferation was modest and predominated with CD8+ cells. No significant correlation was noted between *tax* mRNA load and cell count. On the contrary, there was a trend toward negative correlation between these 2 values. This is reminiscent of the negative effect of Tax expression on cell division observed in nonlymphoid and lymphoid cells that stably express Tax (47, 57). However, *tax* expression was positively correlated with ^{3}H-thymidine incorporation. This conundrum (Tax-triggered thymidine incorporation in the absence of cell division) can be explained in part by the impaired cytokinesis characterizing infected clones expressing *tax*, leading to DNA synthesis and nuclear formation in the absence of cell division.

PBMCs from patients with HAM/TSP proliferate spontaneously in vitro, the percentage of proliferating CD8+ T cells being 2- to 5-fold higher than that of CD4+ T cells (28). Richardson et al. showed that 4 of 12 HTLV-1–positive clones generated by limiting dilution cloning, including 1 of 2 CD8+ clones, underwent spontaneous proliferation that significantly correlated with viral gene expression (19). Here, spontaneous proliferation (i.e., ^{3}H-thymidine incorporation in the absence of IL-2) dramatically increased in HTLV-1–positive clones and was significantly higher in CD8+ than in CD4+ clones. The degree of spontaneous proliferation of uninfected clones deriving from uninfected blood donors was of the same order as that of uninfected clones from HTLV-1–infected individuals. Therefore, the spontaneous polyclonal lymphoproliferation that characterizes PBMCs of patients with HAM/TSP and predominates with CD8+ cells is restricted to the infected subset of lymphocytes without involving uninfected cells.

Tax combines a positive effect on cell cycle with a negative effect on apoptosis (46, 47, 58–61). It inhibits negative cell-cycle regulators such as p53 (62–64), $p16^{INK4A}$ (65–67), and $p27^{Kip1}$ (68) and stimulates positive cell-cycle regulators such as CDK4/6 (61, 69), D-type cyclins (61, 70, 71), and E2F (72; reviewed in ref. 73). Furthermore, Tax suppresses a wide range of factors participating in the apoptotic cascade on the one hand and stimulates factors acting as apoptosis inhibitors on the other (67, 74). The main difference we observed between CD4+ and CD8+ clones corresponded to the mechanisms underlying clonal proliferation ex vivo, i.e., antiapoptosis of CD8+ versus cell cycling of CD4+ lymphocytes. There was no correlation between cell death and *tax* expression, whereas *tax* mRNA load was significantly correlated to the proportion of infected cells in the G_2M and S phases of the cell cycle. These latter findings support the recent molecular demonstrations in the present model of Tax-triggered accumulation of cells in the G_2M and S phases of the cell cycle (75, 76). Thus in the present model, cell cycling but not cell death depended on *tax* expression. The proportion of cells in the S and G_2M phases of the cell cycle significantly correlated with ^{3}H-thymidine incorporation but not with cell counts. This can be explained again by the fact that, in addition to promoting cell cycling, Tax also impairs cytokinesis, leading to DNA synthesis in the absence of cell division.

In conclusion, HTLV-1–infected CD4+ and CD8+ lymphocytes displayed the same pattern of clonal expansion in vivo. Given the similar pattern of replication of both lymphocyte subsets in vivo, why is ATLL regularly of the CD4+ phenotype? The higher degree of in vivo clonal expansion in infected CD4+ lymphocytes might well contribute to selecting malignant events, as a high level of clonal expansion of deltaretrovirus-infected cells is the signature of premalignant clones in vivo (1, 16, 42). Furthermore, ex vivo, infected CD4+ lymphocytes accumulate numerous cellular defects, including multinuclearity, chromatin bridges, and nuclear abnormalities that characterize genetic instability (48–53). One can propose that together with these cellular abnormalities and the extensive oligo/polyclonal expansion observed in vivo, cell cycling, which was restricted to HTLV-1–infected CD4+ untransformed clones in a *tax*-dependent manner, is implicated in promoting HTLV-1–associated lymphoid malignancies and establishes a preleukemic phenotype that is restricted to CD4+ infected cells. By contrast, the CD8+-restricted inhibition of apoptosis, which is independent of *tax* expression, might favor CD8+-dependent control of the infection (20) and inflammatory processes involved in the pathogenesis of HAM/TSP, uveitis, or infective dermatitis. Finally, our present results support that targeting CD4+ cell cycling is of interest in the prevention or treatment of ATLL and that targeting CD8+ antiapoptotic pathways might help prevent or treat HTLV-1–associated inflammatory conditions.

Methods

Samples studied and cell separation. Human PBMCs were obtained after informed consent from 10 patients with HAM/TSP and from 2 uninfected blood donors. Cell separation was achieved by negative selection with the StemSep system using human CD4+ or CD8+ enrichment cocktails as described by the manufacturer (StemCell Technologies).

T cell limiting dilution cloning. PBMCs were cloned in limiting dilution (0.1 cells/well) in Terasaki plates after removal of adherent cells. The medium used for T lymphocytes was RPMI 1640 containing penicillin and streptomycin, sodium pyruvate, nonessential amino acid solution, 2-mercaptoethanol, 10% filtered human AB serum, and 100 U/ml recombinant IL-2 (Chiron Corp.). The cloning medium was the medium used for T lymphocytes supplemented with 1 μg/ml PHA (HA16; Murex Biotech) and 5×10^5 cells/ml irradiated (30 Gy) allogeneic PBMCs (feeder cells). The

Terasaki plates were stored at 37°C for 10 days in aluminum foil and then screened for growing cells under the microscope. Positive cultures were transferred to 96-well U-bottom plates in medium for T lymphocytes and restimulated after a few days. T lymphocytes were restimulated every 14 days with PHA (1 μg/ml) and fresh feeder cells (10^6 cells/ml). Lethally irradiated PBMCs from 3 distinct allogeneic, HTLV-1–negative donors were used as feeder cells to exclude the possibility of clones becoming infected in vitro. To preserve the original growth characteristics of the cells, clones were maintained in this way for no more than 4 months, after which time a fresh aliquot was thawed.

Phenotypic determination. Antibodies recognizing CD4 and CD8 were purchased from Dako. For fluorescence-activated cell scanner (FACS) analysis, PBMCs or cloned T cells were incubated with 5% filtered human serum and then stained with antibodies. Staining and scanning were performed in PBS with 2% FCS. Isotype-matched controls were used. Data were acquired on a FACScan and analyzed by means of CellQuest Pro software (version 4.0.2; BD).

Apoptosis assay. Apoptosis was assessed by using the APOPTEST kit (Dako) containing fluorescein-conjugated annexin V, propidium iodide (PI), and binding buffer. Cells suspended in the binding buffer were mixed with fluorescein-conjugated annexin V and PI. After incubation for 10 minutes, cells were analyzed by FACS. By combining annexin V/FITC and PI, 3 distinct phenotypes could be discriminated: nonapoptotic live cells remained unlabeled, apoptotic cells were labeled by annexin V/FITC, and necrotic cells (necrosis or late apoptosis) were labeled by both annexin V/FITC and PI. Overall, for each sample analyzed, this permitted us to quantify cell viability (annexin V^-PI^-), apoptosis (annexin V^+PI^-), and necrosis (annexin V^+PI^+).

Cell-cycle analysis. Cell-cycle distribution was assessed by measuring the DNA content of a suspension of fresh nuclei by flow cytometric analysis after PI staining. Cloned T cells (5×10^5) were washed with PBS. Supernatant was wasted, and cells were resuspended in 500 μL lysis buffer (0.1% Na citrate, 0.1% Triton X-100, 20 μg/ml PI). After storage at 4°C for a few hours, cells (>10,000) were scanned by flow cytometry and analyzed with ModFit LT software version 2.0 (Verity Software House).

T cell proliferation assay. Proliferation kinetics was assessed by measuring ^{3}H-thymidine incorporation at days 1, 3, 7, 10, and 13. Cells (10^5) were suspended in triplicate in medium containing IL-2 and then pulsed with 1 μCi ^{3}H-thymidine (Amersham Biosciences) for 18 hours. Cells were then harvested, and ^{3}H-thymidine incorporation was measured by liquid scintillation counting. To assess spontaneous proliferation, cells were harvested at day 7 after the sixth PHA stimulation, washed 3 times with PBS, resuspended in growth medium without IL-2, then cultured in triplicate in a 96-well round-bottom plate. After 48 hours, 10^5 cells were pulsed with 1 μCi ^{3}H-thymidine for 18 hours. Cells were then harvested, and ^{3}H-thymidine incorporation was measured by liquid scintillation counting.

p19 antigen ELISA. Cell-free supernatants harvested from T cell clones were analyzed by ELISA using the Retrotek HTLV-I/II p19 Antigen ELISA kit (ZeptoMetrix Corp.) according to the manufacturer's instructions. The concentration of HTLV-1 p19 in specimens was determined by interpolation from a standard curve.

PCRs. T cell clones were screened for HTLV-1 proviral DNA by PCR amplification with long-terminal repeat (LTR) region–specific primers as previously described (77). IPCR amplification of HTLV-1 3′ LTRs and flanking sequences was carried out on the DNA extracted from PBMCs, purified $CD4^+CD8^-$ cells, purified $CD4^-CD8^+$ cells, and cloned T cells as previously described (42). Quantitative measurement of HTLV-1 proviral loads in PBMCs, $CD4^+CD8^-$ and $CD4^-CD8^+$ sorted T cells, and cloned T cells was performed by real-time quantitative PCR as previously described (42). Expression of *tax* was quantified by real-time quantitative RT-PCR as described previously (78). Analysis of TCR γ chain gene rearrangements was performed on DNA extracted from generated clones as previously described (79). This permitted us to confirm the monoclonality of the corresponding cultured cells. Products from multiplex PCR were run on a denaturing gradient gel, which enabled us to detect a band and determine the specific imprint of a given T cell clone if the clone accounted for at least 1% of the total lymphocytes present in the sample.

Statistics. Statistical analysis was performed using the 2-tailed Student's *t* test or the Mann-Whitney *U* rank sum test. The correlations were calculated using the Spearman rank correlation coefficient (ρ). $P < 0.05$ was considered statistically significant in all analyses. All data analyses were performed using SPSS statistical software version 11 (SPSS Inc.).

Acknowledgments

This work was supported by the Ligue Nationale Contre le Cancer (équipe labellisée, 2003), the Centre Léon Bérard, the Centre National pour la Recherche Scientifique, and the Institut National de la Santé et de la Recherche Médicale. D. Sibon was supported by a bursary from the Association pour la Recherche sur le Cancer and from the Fondation pour la Recherche Médicale. S. Rabaaoui and A.-S. Gabet were supported by bursaries from the Centre Léon Bérard. The authors thank Christophe Caux (Centre Léon Bérard), Renaud Mahieux (Institut Pasteur), Patrick Mehlen (Centre Léon Bérard), and Simon Wain-Hobson (Institut Pasteur), for helpful comments. They further thank Marie-Dominique Reynaud for the preparation of the manuscript.

Received for publication October 21, 2005, and accepted in revised form January 10, 2006.

Address correspondence to: Eric Wattel, Oncovirologie et Biothérapies, CNRS UMR5537 — Université Claude Bernard, Centre Léon Bérard 28, rue Laënnec 69373, Lyon Cedex 08, France. Phone: 33-478-78-26-69; Fax: 33-478-78-27-17; E-mail: wattel@lyon.fnclcc.fr.

Anne-Sophie Gabet's present address is: Unit of Infection and Cancer, International Agency for Research on Cancer, World Health Organization, Lyon, France.

Anne-Sophie Gabet and Marc Zandecki contributed equally to this work.

1. Moules, V., et al. 2005. Fate of premalignant clones during the asymptomatic phase preceding lymphoid malignancy. *Cancer Res.* **65**:1234–1243.
2. Yoshida, M. 2001. Multiple viral strategies of Htlv-1 for dysregulation of cell growth control. *Annu. Rev. Immunol.* **19**:475–496.
3. Poiesz, B.J., Ruscetti, F.W., Reitz, M.S., Kalyanaraman, V.S., and Gallo, R.C. 1981. Isolation of a new type C retrovirus (HTLV) in primary uncultured cells of a patient with Sezary T-cell leukemia. *Nature.* **294**:268–271.
4. Kalyanaraman, V.S., et al. 1982. A new subtype of human T-cell leukemia virus (HTLV-II) associated with a T-cell variant of hairy cell leukemia. *Science.* **218**:571–573.
5. Calattini, S., et al. 2005. Discovery of a new human T-cell lymphotropic virus (HTLV-3) in Central Africa. *Retrovirology.* **2**:30.
6. Wolfe, N.D., et al. 2005. Emergence of unique primate T-lymphotropic viruses among central African bushmeat hunters. *Proc. Natl. Acad. Sci. U. S. A.* **102**:7994–7999.
7. Meertens, L., Mahieux, R., Mauclere, P., Lewis, J., and Gessain, A. 2002. Complete sequence of a novel highly divergent simian T-cell lymphotropic virus from wild-caught red-capped mangabeys (Cercocebus torquatus) from Cameroon: a new primate T-lymphotropic virus type 3 subtype. *J. Virol.* **76**:259–268.
8. Ferrer, J.F., Abt, D.A., Bhatt, D.M., and Marshak, R.R. 1974. Studies on the relationship between infection with bovine C-type virus, leukemia, and persistent lymphocytosis in cattle. *Cancer Res.* **34**:893–900.
9. Uchiyama, T., Yodoi, J., Sagawa, K., Takatsuki, K., and Uchino, H. 1977. Adult T-cell leukemia:

clinical and hematologic features of 16 cases. *Blood.* **50**:481–492.
10. Gessain, A., et al. 1985. Antibodies to human T-lymphotropic virus type-I in patients with tropical spastic paraparesis. *Lancet.* **2**:407–410.
11. Nakao, K., Ohba, N., and Matsumoto, M. 1989. Noninfectious anterior uveitis in patients infected with human T- lymphotropic virus type I. *Jpn. J. Ophthalmol.* **33**:472–481.
12. LaGrenade, L., Hanchard, B., Fletcher, V., Cranston, B., and Blattner, W. 1990. Infective dermatitis of Jamaican children: a marker for HTLV-1 infection. *Lancet.* **336**:1345–1347.
13. Jeang, K.T., Giam, C.Z., Majone, F., and Aboud, M. 2004. Life, death, and tax: role of HTLV-1 oncoprotein in genetic instability and cellular transformation. *J. Biol. Chem.* **279**:31991–31994.
14. Furukawa, Y., Osame, M., Kubota, R., Tara, M., and Yoshida, M. 1995. Human T-cell leukemia virus type-1 (HTLV-1) Tax is expressed at the same level in infected cells of HTLV-1-associated myelopathy or tropical spastic paraparesis patients as in asymptomatic carriers but at a lower level in adult T-cell leukemia cells. *Blood.* **85**:1865–1870.
15. Furukawa, Y., Kubota, R., Tara, M., Izumo, S., and Osame, M. 2001. Existence of escape mutant in HTLV-1 tax during the development of adult T-cell leukemia. *Blood.* **97**:987–993.
16. Mortreux, F., Gabet, A.S., and Wattel, E. 2003. Molecular and cellular aspects of HTLV-1 associated leukemogenesis in vivo. *Leukemia.* **17**:26–38.
17. Hollsberg, P., et al. 1992. Characterization of HTLV-1 in vivo infected T cell clones. IL-2- independent growth of nontransformed T cells. *J. Immunol.* **148**:3256–3263.
18. Wucherpfennig, K.W., Hollsberg, P., Richardson, J.H., Benjamin, D., and Hafler, D.A. 1992. T-cell activation by autologous human T-cell leukemia virus type I- infected T-cell clones. *Proc. Natl. Acad. Sci. U. S. A.* **89**:2110–2114.
19. Richardson, J.H., et al. 1997. Variable immortalizing potential and frequent virus latency in blood-derived T-cell clones infected with human T-cell leukemia virus type I. *Blood.* **89**:3303–3314.
20. Hanon, E., et al. 2000. Fratricide among CD8(+) T lymphocytes naturally infected with human T cell lymphotropic virus type I. *Immunity.* **13**:657–664.
21. Nagai, M., Brennan, M.B., Sakai, J.A., Mora, C.A., and Jacobson, S. 2001. CD8(+) T cells are an in vivo reservoir for human T-cell lymphotropic virus type I. *Blood.* **98**:1858–1861.
22. Richardson, J.H., Edwards, A.J., Cruickshank, J.K., Rudge, P., and Dalgleish, A.G. 1990. In vivo cellular tropism of human T-cell leukemia virus type 1. *J. Virol.* **64**:5682–5687.
23. Dahmoush, L., Hijazi, Y., Barnes, E., Stetler-Stevenson, M., and Abati, A. 2002. Adult T-cell leukemia/lymphoma: a cytopathologic, immunocytochemical, and flow cytometric study. *Cancer.* **96**:110–116.
24. Goon, P.K., et al. 2004. Human T cell lymphotropic virus type I (HTLV-I)-specific CD4+ T cells: immunodominance hierarchy and preferential infection with HTLV-1. *J. Immunol.* **172**:1735–1743.
25. Bangham, C.R. 2003. Human T-lymphotropic virus type 1 (HTLV-1): persistence and immune control. *Int. J. Hematol.* **78**:297–303.
26. Jacobson, S. 2002. Immunopathogenesis of human T cell lymphotropic virus type I-associated neurologic disease. *J. Infect. Dis.* **186**(Suppl. 2):S187–S192.
27. Newbound, G.C., Andrews, J.M., O'Rourke, J.P., Brady, J.N., and Lairmore, M.D. 1996. Human T-cell lymphotropic virus type 1 Tax mediates enhanced transcription in CD4+ T lymphocytes. *J. Virol.* **70**:2101–2106.
28. Sakai, J.A., Nagai, M., Brennan, M.B., Mora, C.A., and Jacobson, S. 2001. In vitro spontaneous lymphoproliferation in patients with human T-cell lymphotropic virus type I-associated neurologic disease: predominant expansion of CD8(+) T cells. *Blood.* **98**:1506–1511.
29. Manel, N., et al. 2003. The ubiquitous glucose transporter GLUT-1 is a receptor for HTLV. *Cell.* **115**:449–459.
30. Mortreux, F., Kazanji, M., Gabet, A.S., de Thoisy, B., and Wattel, E. 2001. Two-step nature of human T-cell leukemia virus type 1 replication in experimentally infected squirrel monkeys (Saimiri sciureus). *J. Virol.* **75**:1083–1089.
31. Hoger, T.A., Jacobson, S., Kawanishi, T., Kato, T., Nishioka, K., and Yamamoto, K. 1997. Accumulation of human T lymphotropic virus (HTLV)-I-specific T cell clones in HTLV-I-associated myelopathy/tropical spastic paraparesis patients. *J. Immunol.* **159**:2042–2048.
32. Ureta-Vidal, A., et al. 2001. Human T cell leukemia virus type I (HTLV-1) infection induces greater expansions of CD8 T lymphocytes in persons with HTLV-I-associated myelopathy/tropical spastic paraparesis than in asymptomatic carriers. *J. Infect. Dis.* **183**:857–864.
33. Utz, U., Banks, D., Jacobson, S., and Biddison, W.E. 1996. Analysis of the T-cell receptor repertoire of human T-cell leukemia virus type 1 (HTLV-1) tax-specific CD8+ cytotoxic T lymphocytes from patients with HTLV-1-associated disease: evidence for oligoclonal expansion. *J. Virol.* **70**:843–851.
34. Eiraku, N., et al. 1998. Clonal expansion within CD4+ and CD8+ T cell subsets in human T lymphotropic virus type I-infected individuals. *J. Immunol.* **161**:6674–6680.
35. Gabet, A.S., et al. 2000. High circulating proviral load with oligoclonal expansion of HTLV-1 bearing T cells in HTLV-1 carriers with strongyloidiasis. *Oncogene.* **19**:4954–4960.
36. Cavrois, M., Gessain, A., Wain-Hobson, S., and Wattel, E. 1996. Proliferation of HTLV-1 infected circulating cells in vivo in all asymptomatic carriers and patients with TSP/HAM. *Oncogene.* **12**:2419–2423.
37. Cavrois, M., et al. 1998. Persistent oligoclonal expansion of human T-cell leukemia virus type 1-infected circulating cells in patients with Tropical spastic paraparesis/HTLV-1 associated myelopathy. *Oncogene.* **17**:77–82.
38. Cavrois, M., Wain-Hobson, S., Gessain, A., Plumelle, Y., and Wattel, E. 1996. Adult T-cell leukemia/lymphoma on a background of clonally expanding human T-cell leukemia virus type-1-positive cells. *Blood.* **88**:4646–4650.
39. Etoh, K., et al. 1997. Persistent clonal proliferation of human T-lymphotropic virus type I- infected cells in vivo. *Cancer Res.* **57**:4862–4867.
40. Furukawa, Y., et al. 1992. Frequent clonal proliferation of human T-cell leukemia virus type 1 (HTLV-1)-infected T cells in HTLV-1-associated myelopathy (HAM-TSP). *Blood.* **80**:1012–1016.
41. Leclercq, I., et al. 1998. Oligoclonal proliferation of human T-cell leukaemia virus type 1 bearing T cells in adult T-cell leukaemia/lymphoma without deletion of the 3′ provirus integration sites. *Br. J. Haematol.* **101**:500–506.
42. Mortreux, F., et al. 2001. Somatic mutation in human T-cell leukemia virus type 1 provirus and flanking cellular sequences during clonal expansion in vivo. *J. Natl. Cancer Inst.* **93**:367–377.
43. Wattel, E., Cavrois, M., Gessain, A., and Wain-Hobson, S. 1996. Clonal expansion of infected cells: a way of life for HTLV-1. *J. Acquir. Immune Defic. Syndr. Hum. Retrovirol.* **13**(Suppl. 1):S92–S99.
44. Wattel, E., Vartanian, J.P., Pannetier, C., and Wain-Hobson, S. 1995. Clonal expansion of human T-cell leukemia virus type I-infected cells in asymptomatic and symptomatic carriers without malignancy. *J. Virol.* **69**:2863–2868.
45. Okayama, A., et al. 2004. Role of HTLV-1 proviral DNA load and clonality in the development of adult T-cell leukemia/lymphoma in asymptomatic carriers. *Int. J. Cancer.* **110**:621–625.
46. Liang, M.H., Geisbert, T., Yao, Y., Hinrichs, S.H., and Giam, C.Z. 2002. Human T-lymphotropic virus type 1 oncoprotein tax promotes S-phase entry but blocks mitosis. *J. Virol.* **76**:4022–4033.
47. Sieburg, M., Tripp, A., Ma, J.W., and Feuer, G. 2004. Human T-cell leukemia virus type 1 (HTLV-1) and HTLV-2 tax oncoproteins modulate cell cycle progression and apoptosis. *J. Virol.* **78**:10399–10409.
48. Gisselsson, D., et al. 2001. Abnormal nuclear shape in solid tumors reflects mitotic instability. *Am. J. Pathol.* **158**:199–206.
49. Gisselsson, D., and Hoglund, M. 2005. Connecting mitotic instability and chromosome aberrations in cancer--can telomeres bridge the gap? *Semin. Cancer Biol.* **15**:13–23.
50. Gisselsson, D., et al. 2001. Telomere dysfunction triggers extensive DNA fragmentation and evolution of complex chromosome abnormalities in human malignant tumors. *Proc. Natl. Acad. Sci. U. S. A.* **98**:12683–12688.
51. Gisselsson, D., et al. 2000. Chromosomal breakage-fusion-bridge events cause genetic intratumor heterogeneity. *Proc. Natl. Acad. Sci. U. S. A.* **97**:5357–5362.
52. O'Sullivan, J.N., et al. 2002. Chromosomal instability in ulcerative colitis is related to telomere shortening. *Nat. Genet.* **32**:280–284.
53. Pennarun, G., et al. 2005. Apoptosis related to telomere instability and cell cycle alterations in human glioma cells treated by new highly selective G-quadruplex ligands. *Oncogene.* **24**:2917–2928.
54. Gabet, A.S., et al. 2003. Inactivation of hTERT transcription by tax. *Oncogene.* **22**:3734–3741.
55. Sinha-Datta, U., et al. 2004. Transcriptional activation of hTERT through the NF-kappaB pathway in HTLV-I-transformed cells. *Blood.* **104**:2523–2531.
56. Roth, A., et al. 2005. Telomere loss, senescence, and genetic instability in CD4+ T lymphocytes overexpressing hTERT. *Blood.* **106**:43–50.
57. Jin, D.Y., Spencer, F., and Jeang, K.T. 1998. Human T cell leukemia virus type 1 oncoprotein tax targets the human mitotic checkpoint protein MAD1. *Cell.* **93**:81–91.
58. Haoudi, A., and Semmes, O.J. 2003. The HTLV-1 tax oncoprotein attenuates DNA damage induced G1 arrest and enhances apoptosis in p53 null cells. *Virology.* **305**:229–239.
59. Jeang, K.T., Widen, S.G., Semmes, O.J., 4th, and Wilson, S.H. 1990. HTLV-1 trans-activator protein, tax, is a trans-repressor of the human beta-polymerase gene. *Science.* **247**:1082–1084.
60. Neuveut, C., and Jeang, K.T. 2002. Cell cycle dysregulation by HTLV-1: role of the tax oncoprotein. *Front. Biosci.* **7**:D157–D163.
61. Neuveut, C., et al. 1998. Human T-cell leukemia virus type 1 Tax and cell cycle progression: role of cyclin D-cdk and p110Rb. *Mol. Cell. Biol.* **18**:3620–3632.
62. Pise-Masison, C.A., et al. 1998. Inhibition of p53 transactivation function by the human T-cell lymphotropic virus type 1 Tax protein. *J. Virol.* **72**:1165–1170.
63. Cereseto, A., et al. 1996. p53 functional impairment and high p21waf1/cip1 expression in human T- cell lymphotropic/leukemia virus type I-transformed T cells. *Blood.* **88**:1551–1560.
64. Mulloy, J.C., et al. 1998. Human T-cell lymphotropic/leukemia virus type 1 tax abrogates p53-induced cell cycle arrest and apoptosis through its CREB/ATF functional domain. *J. Virol.* **72**:8852–8860.
65. Suzuki, T., Narita, T., Uchida-Toita, M., and Yoshida, M. 1999. Down-regulation of the INK4 family of cyclin-dependent kinase inhibitors by tax protein of HTLV-1 through two distinct mechanisms. *Virology.* **259**:384–391.

66. Suzuki, T., Kitao, S., Matsushime, H., and Yoshida, M. 1996. HTLV-1 Tax protein interacts with cyclin-dependent kinase inhibitor p16INK4A and counteracts its inhibitory activity towards CDK4. *EMBO J.* **15**:1607–1614.
67. Low, K.G., et al. 1997. Human T-cell leukemia virus type 1 tax releases cell cycle arrest induced by p16INK4a. *J. Virol.* **71**:1956–1962.
68. Cereseto, A., Washington Parks, R., Rivadeneira, E., and Franchini, G. 1999. Limiting amounts of p27Kip1 correlates with constitutive activation of cyclin E-CDK2 complex in HTLV-I-transformed T-cells. *Oncogene.* **18**:2441–2450.
69. Schmitt, I., Rosin, O., Rohwer, P., Gossen, M., and Grassmann, R. 1998. Stimulation of cyclin-dependent kinase activity and G1- to S-phase transition in human lymphocytes by the human T-cell leukemia/lymphotropic virus type 1 Tax protein. *J. Virol.* **72**:633–640.
70. Akagi, T., Ono, H., and Shimotohno, K. 1996. Expression of cell-cycle regulatory genes in HTLV-1 infected T-cell lines: possible involvement of Tax1 in the altered expression of cyclin D2, p18Ink4 and p21Waf1/Cip1/Sdi1. *Oncogene.* **12**:1645–1652.
71. Santiago, F., et al. 1999. Transcriptional up-regulation of the cyclin D2 gene and acquisition of new cyclin-dependent kinase partners in human T-cell leukemia virus type 1-infected cells. *J. Virol.* **73**:9917–9927.
72. Ohtani, K., et al. 2000. Cell type-specific E2F activation and cell cycle progression induced by the oncogene product Tax of human T-cell leukemia virus type I. *J. Biol. Chem.* **275**:11154–11163.
73. Mesnard, J.M., and Devaux, C. 1999. Multiple control levels of cell proliferation by human T-cell leukemia virus type 1 Tax protein. *Virology.* **257**:277–284.
74. Kawakami, A., et al. 1999. Inhibition of caspase cascade by HTLV-1 tax through induction of NF- kappaB nuclear translocation. *Blood.* **94**:3847–3854.
75. Haoudi, A., Daniels, R.C., Wong, E., Kupfer, G., and Semmes, O.J. 2003. Human T-cell leukemia virus-I tax oncoprotein functionally targets a subnuclear complex involved in cellular DNA damage-response. *J. Biol. Chem.* **278**:37736–37744.
76. Liu, B., Hong, S., Tang, Z., Yu, H., and Giam, C.Z. 2005. HTLV-1 Tax directly binds the Cdc20-associated anaphase-promoting complex and activates it ahead of schedule. *Proc. Natl. Acad. Sci. U. S. A.* **102**:63–68.
77. Saito, M., et al. 1996. Mutation rates in LTR of HTLV-1 in HAM/TSP patients and the carriers are similarly high to Tax/Rex-coding sequence. *J. Neurovirol.* **2**:330–335.
78. Yamano, Y., et al. 2004. Increased expression of human T lymphocyte virus type I (HTLV-1) Tax11-19 peptide-human histocompatibility leukocyte antigen A*201 complexes on CD4+ CD25+ T cells detected by peptide-specific, major histocompatibility complex-restricted antibodies in patients with HTLV-I-associated neurologic disease. *J. Exp. Med.* **199**:1367–1377.
79. Theodorou, I., et al. 1996. VJ rearrangements of the TCR gamma locus in peripheral T-cell lymphomas: analysis by polymerase chain reaction and denaturing gradient gel electrophoresis. *J. Pathol.* **178**:303–310.